International Journal of Heat and Mass Transfer 52 (2009) 112–123

Contents lists available at ScienceDirect

International Journal of Heat and Mass Transfer

journal homepage: www.elsevier.com/locate/ijhmt

Hybrid formulation and solution for transient conjugated conduction–external convection

C.P. Naveira [a], M. Lachi [b], R.M. Cotta [a,*], J. Padet [b]

[a] Mechanical Engineering Department, POLI & COPPE, Universidade Federal do Rio de Janeiro, Cidade Universitária, Cx. Postal 68503, Rio de Janeiro, RJ 21945-970, Brazil
[b] Laboratoire de Thermomécanique, UTAP, Université de Reims, France

ARTICLE INFO

Article history:
Received 27 February 2008
Received in revised form 31 May 2008
Available online 3 August 2008

Keywords:
Conjugated problems
Hybrid methods
Integral transforms
Boundary layer
External convection

ABSTRACT

This work presents a hybrid numerical–analytical solution for transient laminar forced convection over flat plates of non-negligible thickness, subjected to arbitrary time variations of applied wall heat flux at the fluid–solid interface. This conjugated conduction–convection problem is first reformulated through the employment of the coupled integral equations approach (CIEA) to simplify the heat conduction problem on the plate by averaging the related energy equation in the transversal direction. As a result, an improved lumped partial differential formulation for the transversally averaged wall temperature is obtained, while a third kind boundary condition is achieved for the fluid from the heat balance at the solid–fluid interface. From the available steady velocity distributions, a hybrid numerical–analytical solution based on the generalized integral transform technique (GITT), under its partial transformation mode, is then proposed, combined with the method of lines implemented in the *Mathematica* 5.2 routine *NDSolve*. The interface heat flux partitions and heat transfer coefficients are readily determined from the wall temperature distributions, as well as the temperature values at any desired point within the fluid. A few test cases for different materials and wall thicknesses are defined to allow for a physical interpretation of the wall participation effect in contrast with the simplified model without conjugation.

1. Introduction

New perspectives have been opened by hybrid numerical–analytical approaches that attempt to incorporate the advantages associated with the classical analytical approaches, while offering sufficient flexibility for dealing with more than just model equations, and aiming at providing a feasible alternative to the purely discrete approaches in a significant range of applications. One such hybrid approach is the so-called generalized integral transform technique (GITT) [1–5], which extends the classical integral transform analytical approach towards the hybrid analysis of linear and nonlinear diffusion and convection–diffusion problems, and has been applied to a number of problems in heat and fluid flow. Within the context of solving the boundary layer equations with the GITT, most previous contributions are related to internal flow problems, but it is worth noting a few previous works concerned with external flow situations [6–8]. The basic concept is to propose eigenfunction expansions to the dependent variables based on the diffusion operator's behavior, and perform the integral transformation of the related partial differential equations. One may propose expansions in all but one independent variable, and then the integral transformation procedure results in a coupled system of ordinary differential equations for the transformed potentials, to be, in general, numerically handled along this single remaining independent variable not eliminated through the integration. This is named the total transformation mode of the GITT approach, and has been the most frequently adopted along the last few decades. Another possibility, which has been more intensively employed in recent years, is the so-called partial transformation mode [1,7–10], in which not just one independent variable remains, when the user might choose not to propose the expansion in all spatial variables, for instance. Then, a coupled system of partial differential equations results for the transformed potentials, in terms, usually, of the two independent variables chosen not to be eliminated by integral transformation. This approach is particularly useful in parabolic–hyperbolic formulations, when the diffusion operator might not be present in one of the spatial variables. Such is the case in the present class of problems, related to the boundary layer formulation for the energy equation in transient state, when the diffusion operator in the longitudinal direction is normally disregarded.

Convective heat transfer over surfaces or within channels may be handled under the boundary layer formulation for a wide range of practical situations. Such interest has justified the previous efforts towards the hybrid numerical–analytical treatment of heat and fluid flow boundary layers by integral transforms in light of the inherent difficulties in obtaining exact analytical solutions to this class of problems. Of particular interest to the present

* Corresponding author.
E-mail address: cotta@mecanica.coppe.ufrj.br (R.M. Cotta).

0017-9310/$ - see front matter © 2008 Elsevier Ltd. All rights reserved.
doi:10.1016/j.ijheatmasstransfer.2008.05.034

Nomenclature

$h(x,t)$	heat transfer coefficient at interface (W/m^2 °C)
k_f	thermal conductivity (fluid) (W m^{-1} K^{-1})
k_s	thermal conductivity (solid) (W m^{-1} K^{-1})
L	plate length (m)
Pe	Peclet number
Q_w	dimensionless imposed interface heat flux
Re_L	Reynolds number
t	time variable (s)
T_∞	free stream temperature (°C)
T_f	fluid temperature (°C)
T_s	solid temperature (°C)
T_{av}	averaged wall temperature (°C)
u_∞	free stream velocity (m s^{-1})
u	longitudinal velocity component (m s^{-1})
U	dimensionless longitudinal velocity component
v	transversal velocity component (m s^{-1})
V	dimensionless transversal velocity component
x^*	longitudinal coordinate (m)
x	dimensionless longitudinal coordinate
y^*	transversal coordinate (m)
y	dimensionless transversal coordinate

Greek letters

α_f	thermal diffusivity (fluid) (m^2 s^{-1})
α_s	thermal diffusivity (solid) (m^2 s^{-1})
χ	dimensionless transformed longitudinal coordinate
η_t	dimensionless transformed transversal coordinate
$\delta^*(x^*)$	velocity boundary layer thickness (m)
$\delta(\chi)$	dimensionless velocity boundary layer thickness
$\delta_t^*(x^*,t)$	thermal boundary layer thickness (m)
$\delta_t(\chi)$	dimensionless thermal boundary layer thickness
θ_f	dimensionless temperature (fluid)
θ_{av}	dimensionless averaged wall temperature (solid)
ν	kinematic viscosity (m^2 s^{-1})
τ	dimensionless time
$\phi(t)$	imposed interface heat flux (W/m^2)
ϕ_{ref}	reference heat flux at interface (W/m^2)

contribution is the recent analysis of transient convective heat transfer over flat plates, handled under the partial integral transformation mode of the GITT approach [8]. From the availability of the velocity field, the fluid energy equation is integral transformed in the transversal direction, yielding a partial differential formulation in terms of time and longitudinal coordinate. The transformed formulation is then numerically handled, as inherent to this so-called partial transformation mode. Such hybrid solution was then critically compared against the approximate solution by the classical integral method for the transient boundary layer equations [11], which in fact allowed for the benchmarking of the classical Karman–Pohlhausen approach for the transient situation.

Conjugated conduction–convection problems are among the classical formulations in heat transfer that still demand exact analytical treatment, since the pioneering work of Perelman [12] and Luikov et al. [13,14], while deserving the attention of various researchers towards the development of approximate formulations and/or solutions, either in external or internal flow situations. The main mathematical difficulties in exactly handling this class of problems are related with the coupled multiregion spectral analysis required, together with the mixed elliptic (wall) and parabolic (fluid) natures of the partial differential system. For the situation of external flow being addressed in the present investigation, a number of contributions were made available dealing with the steady-state situation [15–20], including both closed form approximate expressions and numerical solutions of the coupled fluid and solid energy equations. The present integral transform approach itself has been applied to obtain hybrid solutions for conjugated conduction–convection problems [21–23], in both steady and periodic formulations, but only for the internal flow situation, by employing a transversally lumped heat conduction equation for the wall temperature. Finally, a few recent contributions have addressed the fully transient external flow situation, offering approximate solutions to both the fluid and solid coupled temperature distributions [24–27].

The present work brings further contribution to the hybrid numerical–analytical solution of conjugated conduction–external convection problems, for either steady or transient formulations. Incompressible steady laminar flow over a flat plate of non-negligible thickness is thus considered, and the temperature transients are caused by the time variation of the heat flux applied directly at the fluid–solid interface. The proposed formulation is motivated by the flash experimental method for the determination of thermophysical properties and/or heat transfer coefficients [28,29], when the surface of the plate exposed to the flowing fluid is irradiated by a flash lamp and the heat absorbed by the illuminated wall represents the imposed interface heat flux. The solution is pursued by first reformulating the wall heat conduction problem, adopting an improved lumped model based on the coupled integral equations approach (CIEA) [2,30–32]. Thus, the transient energy equation for the solid is integrated in the transversal direction, and employing Hermite approximations for integrals [2], a more accurate relationship between the interface and the solid average temperatures is established, as compared to the classical lumped system analysis. As a result, a third type boundary condition for the fluid temperature problem is reached. The energy equation for the fluid is then integral transformed, eliminating the transversal direction from the problem formulation, which is later analytically recovered by the explicit inversion formula. The resulting coupled partial differential system for the transversally averaged solid temperature and for the transformed fluid temperatures is then numerically handled, making use of the Method of Lines implemented in the function *NDSolve* of the *Mathematica* 5.2 software system [33].

Numerical results are then obtained for quantities of practical interest, such as heat transfer coefficients and the heat flux partition between the fluid and the participating solid. Five cases for different choices of material and wall thickness were considered more closely, to illustrate the conjugation effects in comparison against the base case without wall participation and among themselves.

2. Problem formulation

The considered problem involves laminar incompressible flow of a Newtonian fluid over a flat plate, with steady-state flow but transient convective heat transfer due to a time variable applied heat flux, $\phi(t)$, at the solid–fluid interface. The fluid flows with a free stream velocity u_∞, which arrives at the plate front edge at the temperature T_∞ (Fig. 1). The wall is considered to participate on the heat transfer problem, with thickness, e, length, L, and related thermophysical properties. The boundary layer equations are assumed to be valid for the flow and heat transfer problem within the fluid, and the conjugated conduction–external convection problem is written as:

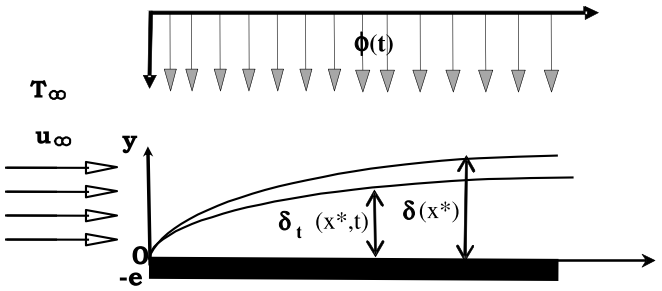

Fig. 1. Description of physical problem and coordinates system for transient conjugated conduction–external convection for laminar flow over a flat plate.

Continuity:

$$\frac{\partial u(x^*,y^*)}{\partial x^*}+\frac{\partial v(x^*,y^*)}{\partial y^*}=0,\qquad 0<y^*<\delta^*(x^*),\quad 0<x^*<L \tag{1}$$

Momentum in x-direction:

$$u\frac{\partial u}{\partial x^*}+v\frac{\partial u}{\partial y^*}=\nu\frac{\partial^2 u}{\partial y^{*2}},\qquad 0<y^*<\delta^*(x^*),\quad 0<x^*<L \tag{2}$$

Fluid and solid energy equations:

$$\frac{\partial T_f(x^*,y^*,t)}{\partial t}+u\frac{\partial T_f(x^*,y^*,t)}{\partial x^*}+v\frac{\partial T_f(x^*,y^*,t)}{\partial y^*}=\alpha_f\frac{\partial^2 T_f(x^*,y^*,t)}{\partial y^{*2}},\quad 0<y^*<\delta_t^*(x^*,t),\quad 0<x^*<L,\quad t>0 \tag{3}$$

$$\frac{\partial T_s(x^*,y^*,t)}{\partial t}=\alpha_s\left(\frac{\partial^2 T_s(x^*,y^*,t)}{\partial x^{*2}}+\frac{\partial^2 T_s(x^*,y^*,t)}{\partial y^{*2}}\right),\quad -e<y^*<0,\quad 0<x^*<L,\quad t>0 \tag{4}$$

with initial conditions

$$T_f(x^*,y^*,0)=T_\infty,\qquad 0<y^*<\infty,\quad 0<x^*<L \tag{5}$$

$$T_s(x^*,y^*,0)=T_\infty,\qquad -e<y^*<0,\quad 0<x^*<L \tag{6}$$

and boundary and interface conditions:

$$T_f(x^*,\delta_t^*,t)=T_\infty,\quad 0<x^*<L,\ t>0 \tag{7}$$

$$T_f(x^*,0,t)=T_s(x^*,0,t),\quad 0<x^*<L,\ t>0 \tag{8}$$

$$-k_f\left.\frac{\partial T_f}{\partial y^*}\right|_{y^*=0}=-k_s\left.\frac{\partial T_s}{\partial y^*}\right|_{y^*=0}+\phi(t),\quad 0<x^*<L,\ t>0 \tag{9}$$

$$-k_s\left.\frac{\partial T_s}{\partial y^*}\right|_{y^*=-e}=0,\quad 0<x^*<L,\ t>0 \tag{10}$$

$$T_f(0,y^*,t)=T_\infty,\quad 0<y^*<\infty,\ t>0 \tag{11}$$

$$\left.\frac{\partial T_s}{\partial x^*}\right|_{x^*=0}=\left.\frac{\partial T_s}{\partial x^*}\right|_{x^*=L}=0,\quad -e<y^*<0,\ t>0 \tag{12}$$

The boundary layer flow problem solution is considered known at this point, by a chosen approximate analytical or numerical solution technique, subjected to the usual boundary conditions of no-slip and impermeability at the wall and free stream conditions at a distance sufficiently away from the plate [34].

The proposed thermal problem, Eqs. (3)–(12), may be simplified through the proposition of a lumped formulation for the wall, integrating its temperature field along the transversal direction, y^*. Here, instead of employing the Classical Lumped System Analysis, which essentially assumes the wall temperature field to be uniform in the transversal direction, a more refined improved model is proposed. The CIEA [2,30–32] is a very straightforward reformulation tool employed in the simplification of diffusion or convection–diffusion problems via averaging processes in one or more of the involved space variables. Simpler formulations of the original partial differential systems are obtained, through a reduction of the number of independent variables in multidimensional situations, by integration (averaging) of the full partial differential equations in one or more space variables, but retaining some information in the direction integrated out, provided by the related boundary conditions. Different levels of approximation in such mixed lumped-differential formulations can be used, starting from the plain and classical lumped system analysis, towards improved formulations, obtained through Hermite-type approximations for integrals [2]. Based on the values of the integrand and its derivatives at the integration limits, such approximations are given in the form:

$$\int_{x_{i-1}}^{x_i} y(x)\,dx\cong\sum_{v=0}^{\alpha}C_v y_{i-1}^{(v)}+\sum_{v=0}^{\beta}D_v y_i^{(v)} \tag{13}$$

where $y(x)$ and its derivatives $y^{(v)}(x)$ are defined for all $x\in(x_{i-1},x_i)$. Furthermore, it is assumed that the numerical values of $y^{(v)}(x_{i-1})\equiv y_{i-1}^{(v)}$ for $v=0,1,2,\ldots,\alpha$ and $y^{(v)}(x_i)\equiv y_i^{(v)}$ for $v=0,1,2,\ldots,\beta$, are available at the end points of the interval. In such a manner, the integral of $y(x)$ is expressed as a linear combination of $y(x_{i-1})$, $y(x_i)$ and their derivatives, $y^{(v)}(x_{i-1})$ up to order $v=\alpha$, and $y^{(v)}(x_i)$ up to order $v=\beta$. The resulting expression for this so-called $H_{\alpha,\beta}$-approximation is given by:

$$\int_{x_{i-1}}^{x_i} y(x)\,dx=\sum_{v=0}^{\alpha}C_v(\alpha,\beta)h_i^{v+1}y_{i-1}^{(v)}+\sum_{v=0}^{\beta}C_v(\beta,\alpha)(-1)^v h_i^{v+1}y_i^{(v)}+O(h_i^{\alpha+\beta+3}) \tag{14}$$

where,

$$h_i=x_i-x_{i-1},\quad C_v(\alpha,\beta)=\frac{(\alpha+1)!(\alpha+\beta+1-v)!}{(v+1)!(\alpha-v)!(\alpha+\beta+2)!} \tag{15}$$

In the present work, we consider just the two approximations, $H_{0,0}$ and $H_{1,1}$, which correspond, respectively, to the well-known trapezoidal and corrected trapezoidal integration rules, given by:

$$H_{0,0}\rightarrow\int_0^h y(x)\,dx\cong\frac{h}{2}(y(0)+y(h)) \tag{16}$$

$$H_{1,1}\rightarrow\int_0^h y(x)\,dx\cong\frac{h}{2}(y(0)+y(h))+\frac{h^2}{12}(y'(0)-y'(h)) \tag{17}$$

According to this approach, the transversally averaged wall temperature is to be approximated by a Hermite formula for integrals, here by taking the $H_{1,1}$ approximation, the corrected trapezoidal rule. In addition, the transversally averaged wall heat flux shall be approximated by the simplest $H_{0,0}$ approximation, the trapezoidal rule. This $H_{1,1}/H_{0,0}$ combined solution does not change the nature of the problem in comparison with the classical lumped formulation, but only modifies the equation coefficients. Nevertheless, it has been shown to be significantly more accurate than the classical lumped system analysis in the applicable range of the governing parameters [2]. From the physical point of view, the present approach generalizes the concept of the lumped system analysis, by accounting for the contribution of the boundaries temperatures and heat fluxes in estimating the average temperature and wall heat flux within the medium (here across the plate thickness only). Thus, the CIEA avoids the assumption that the average temperature is equal to the boundary value as in the classical lumped approach, which in fact corresponds to a plain rectangle integration formula for the average temperature approximation, without consideration of the temperature and heat flux variation across the medium.

The transversally averaged wall temperature, $T_{av}(x^*,t)$, is thus approximated by the CIEA as:

$$T_{av}(x^*,t)\equiv\frac{1}{e}\int_{-e}^{0}T_s(x^*,y^*,t)\,dy\approx\frac{1}{2}[T_s(x^*,0,t)+T_s(x^*,-e,t)]-\frac{e}{12}\left.\frac{\partial T_s}{\partial y^*}\right|_{y^*=0} \tag{18}$$

The average heat flux is approximated as:

$$\int_{-e}^{0}\frac{\partial T_s(x^*,y^*,t)}{\partial y^*}\,dy^* \equiv [T_s(x^*,0,t)-T_s(x^*,-e,t)] \approx \frac{e}{2}\left.\frac{\partial T_s}{\partial y^*}\right|_{y^*=0} \quad (19)$$

An expression for the temperature at $y^* = -e$, is then obtained:

$$T_s(x^*,-e,t) = 2T_{av}(x^*,t) - T_s(x^*,0,t) + \frac{e}{6}\left.\frac{\partial T_s}{\partial y^*}\right|_{y^*=0} \quad (20)$$

This expression is substituted into the average heat flux expression, Eq. (19), providing:

$$\left[T_s(x^*,0,t) - \left(2T_{av}(x^*,t) - T_s(x^*,0,t) + \frac{e}{6}\left.\frac{\partial T_s}{\partial y^*}\right|_{y^*=0}\right)\right] = \frac{e}{2}\left.\frac{\partial T_s}{\partial y^*}\right|_{y^*=0} \quad (21)$$

Then, the interface condition, Eq. (8), is recalled, yielding:

$$\left.\frac{\partial T_s}{\partial y^*}\right|_{y^*=0} = \frac{3}{e}[T_f(x^*,0,t) - T_{av}(x^*,t)] \quad (22)$$

and the interface condition, Eq. (9), is now reformulated as:

$$-k_f\left.\frac{\partial T_f}{\partial y^*}\right|_{y^*=0} = \phi(t) - \frac{3k_s}{e}[T_f(x^*,0,t) - T_{av}(x^*,t)] \quad (23)$$

Clearly, according to the above expression, the boundary condition for the fluid at $y^* = 0$ was reformulated as a third kind boundary condition that includes the participation of the wall through its averaged temperature. When the interface temperature, $T_f(x^*,0,t)$, and the average solid temperature, $T_{av}(x^*,t)$, have the same value, the wall does not participate and the conventional second kind boundary condition for an imposed heat flux is recovered.

The energy equation for the solid is now reformulated by taking the average on the transversal direction, operating with $\frac{1}{e}\int_{-e}^{0}\_\_\_dy^*$, to yield:

$$\begin{aligned}\frac{\partial T_{av}(x^*,t)}{\partial t} &= \alpha_s\frac{\partial^2 T_{av}(x^*,t)}{\partial x^{*2}} + \frac{\alpha_s}{e}\int_{-e}^{0}\frac{\partial^2 T_s(x^*,y^*,t)}{\partial y^{*2}}\,dy^* \\ &= \alpha_s\frac{\partial^2 T_{av}(x^*,t)}{\partial x^{*2}} + \frac{\alpha_s}{e}\left[\left.\frac{\partial T_s(x^*,y^*,t)}{\partial y^*}\right|_{y^*=0} - \left.\frac{\partial T_s(x^*,y^*,t)}{\partial y^*}\right|_{y^*=-e}\right]\end{aligned} \quad (24)$$

We can then eliminate the derivatives at $y^* = 0$ and at $y^* = -e$ by applying the interface conditions, Eqs. (9) and (10):

$$\frac{\partial T_{av}(x^*,t)}{\partial t} = \alpha_s\frac{\partial^2 T_{av}(x^*,t)}{\partial x^{*2}} + \frac{\alpha_s}{ek_s}\left[k_f\left.\frac{\partial T_f(x^*,y^*,t)}{\partial y^*}\right|_{y^*=0} + \phi(t)\right] \quad (25)$$

or, by recalling the reformulated fluid boundary condition:

$$\frac{\partial T_{av}(x^*,t)}{\partial t} = \alpha_s\frac{\partial^2 T_{av}(x^*,t)}{\partial x^{*2}} - \frac{3\alpha_s}{e^2}[T_{av}(x^*,t) - T_f(x^*,0,t)] \quad (26)$$

This lumped-differential equation is complemented by the also averaged initial and boundary conditions:

$$T_{av}(x^*,0) = T_\infty \quad (27)$$

$$\left.\frac{\partial T_{av}(x^*,t)}{\partial x^*}\right|_{x^*=0} = 0; \quad \left.\frac{\partial T_{av}(x^*,t)}{\partial x^*}\right|_{x^*=L} = 0 \quad (28)$$

Again, the difference between the average solid temperature and the fluid interface temperature is responsible for the coupling of the two processes along the longitudinal coordinate, x^*.

Higher order formulations could be achieved but then the nature of the formulation would somehow change. For instance, by introducing the $H_{1,1}$ approximation also for the average heat flux, the formulation would then incorporate a partial differential equation for the temperature at $y^* = -e$, which is not entirely eliminated, coupled to the average wall and interface temperatures. We have here preferred to obtain a simpler formulation for the conjugated problem as above described. The conjugated conduction–convection problem can also be rewritten after introducing the following dimensionless variables:

$$\begin{aligned}&U = \frac{u}{u_\infty}, \quad V = \frac{v}{u_\infty}, \quad x = \frac{x^*}{L}, \quad y = \frac{y^*}{L}, \quad \tau = \frac{u_\infty\cdot t}{L}, \\ &\theta = \frac{T-T_\infty}{\frac{\phi_{ref}\cdot L}{k_f}}, \quad Re_L = \frac{u_\infty\cdot L}{\nu}, \quad Pe_f = \frac{u_\infty\cdot L}{\alpha_f}, \\ &Pe_s = \frac{u_\infty\cdot e}{\alpha_s}, \quad \delta = \frac{\delta^*}{L}, \quad \delta_t = \frac{\delta_t^*}{L}, \quad Q_w = \frac{\phi}{\phi_{ref}}, \\ &R = \frac{e}{L}, \quad K = \frac{k_f}{k_s}\end{aligned} \quad (29)$$

and the governing dimensionless equations for the flow problem are given by:

$$\frac{\partial U(x,y)}{\partial x} + \frac{\partial V(x,y)}{\partial y} = 0, \qquad 0 < y < \delta(x), \quad 0 < x < 1 \quad (30)$$

$$U\frac{\partial U}{\partial x} + V\frac{\partial U}{\partial y} = \frac{1}{Re_L}\frac{\partial^2 U}{\partial y^2}, \qquad 0 < y < \delta(x), \quad 0 < x < 1 \quad (31)$$

The thermal problem is essentially confined to a region here represented by the time-independent thickness $\delta_t(x)$, which just needs to be large enough to encompass the actual thermally affected region throughout the transient process. In applying the integral transform approach [1–5], we are by no means constrained to finding a transient thermal boundary layer thickness and the formulation is essentially treated as that for a semi-infinite region. However, it is of interest to avoid the proposition of eigenfunction expansions with variable eigenvalues along the longitudinal coordinate. Therefore, we introduce a domain regularization transformation for the spatial domain written as:

$$\eta_t = \frac{y}{\delta_t(x)} \quad \text{and} \quad \chi = x \quad (32)$$

Then, the dimensionless form for the fluid energy equation after the domain transformation is given by:

$$\delta_t^2(\chi)\frac{\partial\theta_f(\chi,\eta_t,\tau)}{\partial\tau} + U^*\frac{\partial\theta_f(\chi,\eta_t,\tau)}{\partial\chi} + V^*\frac{\partial\theta_f(\chi,\eta_t,\tau)}{\partial\eta_t} = \frac{1}{Pe_f}\frac{\partial^2\theta_f(\chi,\eta_t,\tau)}{\partial\eta_t^2}, \quad 0<\eta_t<1, \quad 0<\chi<1, \quad \tau>0 \quad (33)$$

where

$$\begin{aligned}&U^*(\chi,\eta_t) = U(\chi,\eta_t)\delta_t^2(\chi) \quad \text{and} \\ &V^*(\chi,\eta_t) = \eta_t U(\chi,\eta_t)\delta_t(\chi)\frac{d\delta_t(\chi)}{d\chi} + V(\chi,\eta_t)\delta_t(\chi)\end{aligned} \quad (34)$$

The initial and boundary conditions become:

$$\theta_f(\chi,\eta_t,0) = 0, \qquad 0<\eta_t<1, \quad 0<\chi<1 \quad (35)$$

$$\theta_f(0,\eta_t,\tau) = 0, \qquad 0<\eta_t<1, \quad \tau>0 \quad (36)$$

$$\theta_f(\chi,1,\tau) = 0, \qquad 0<\chi<1, \quad \tau>0 \quad (37)$$

$$\left.\frac{\partial\theta_f}{\partial\eta_t}\right|_{\eta_t=0} = \frac{3\delta_t(\chi)}{K\cdot R}[\theta_f(\chi,0,\tau) - \theta_{av}(\chi,\tau)] - \delta_t(\chi)Q_w(\tau), \quad 0<\chi<1, \quad \tau>0 \quad (38)$$

And the wall energy equation with the respective initial and boundary conditions are given by:

$$\frac{\partial\theta_{av}(\chi,\tau)}{\partial\tau} = \frac{R}{Pe_s}\frac{\partial^2\theta_{av}(\chi,\tau)}{\partial\chi^2} + \frac{3}{Pe_s\cdot R}[\theta_f(\chi,0,\tau) - \theta_{av}(\chi,\tau)], \qquad 0<\chi<1, \quad \tau>0 \quad (39)$$

$$\theta_{av}(\chi,0)=0,\quad 0<\chi<1 \tag{40}$$

$$\left.\frac{\partial\theta_{av}}{\partial\chi}\right|_{\chi=0}=\left.\frac{\partial\theta_{av}}{\partial\chi}\right|_{\chi=1}=0,\quad \tau>0 \tag{41}$$

3. Solution methodology

The flow problem is readily solved according to Blasius similarity transformation [34], which provides the velocity components to feed into the decoupled transient energy equation. For the thermal problem solution, since there is a preferential convective direction aligned with the flow, the integral transformation was chosen to be operated solely in the transversal direction, along which diffusion predominates. However, Eqs. (5)–(9) are still not in the most convenient form for integral transformation, since the boundary condition at the wall involves a non-homogeneous term at $\eta_t = 0$, which might be responsible for a slow convergence behavior of the eigenfunction expansion, especially in the vicinity of this boundary source term. A filtering solution is then proposed, so as to eliminate the non-homogeneous boundary condition, in the form:

$$\theta_f(\chi,\eta_t,\tau)=\theta_f^*(\chi,\eta_t,\tau)+F(\eta_t;\chi,\tau) \tag{42}$$

Here, a straightforward second-degree polynomial filter is proposed, $F(\eta_t;\chi,\tau)$, where χ and τ are just parameters of the solution. The filter is obtained from satisfaction of the three essential boundary conditions at the transversal domain edges:

$$\begin{aligned}&F(\eta_t;\chi,\tau)=e_0(\chi,\tau)+e_1(\chi,\tau)\eta_t+e_2(\chi,\tau)\eta_t^2,\quad 0<\chi<1,\quad 0<\eta_t<1,\quad \tau>0\\ &F(1;\chi,\tau)=0\qquad \left.\frac{dF}{d\eta_t}\right|_{\eta_t=1}=0\\ &\left.\frac{dF}{d\eta_t}\right|_{\eta_t=0}=3\delta_t(\chi)\frac{1}{KR}[F(0;\chi,\tau)-\theta_{av}(\chi,\tau)]-\delta_t(\chi)Q_w(\tau)\end{aligned} \tag{43}$$

Thus, applying the proposed filtering solution to Eq. (33), the resulting filtered problem is given by:

$$\begin{aligned}&\delta_t^2(\chi)\frac{\partial\theta_f^*(\chi,\eta_t,\tau)}{\partial\tau}+U^*\frac{\partial\theta_f^*(\chi,\eta_t,\tau)}{\partial\chi}+V^*\frac{\partial\theta_f^*(\chi,\eta_t,\tau)}{\partial\eta_t}\\ &\quad=\frac{1}{Pe_f}\frac{\partial^2\theta_f^*(\chi,\eta_t,\tau)}{\partial\eta_t^2}+G(\chi,\eta_t,\tau),\\ &\quad 0<\eta_t<1,\quad 0<\chi<1,\quad \tau>0\end{aligned} \tag{44}$$

where

$$\begin{aligned}G(\chi,\eta_t,\tau)=&-\delta_t^2(\chi)\frac{\partial F(\eta_t;\chi,\tau)}{\partial\tau}-U^*\frac{\partial F(\eta_t;\chi,\tau)}{\partial\chi}-V^*\frac{\partial F(\eta_t;\chi,\tau)}{\partial\eta_t}\\ &+\frac{1}{Pe_f}\frac{\partial^2F(\eta_t;\chi,\tau)}{\partial\eta_t^2}\end{aligned} \tag{45}$$

with initial and boundary conditions:

$$\theta_f^*(\chi,\eta_t,0)=-F(\eta_t;\chi,0),\qquad 0<\chi<1,\quad 0<\eta_t<1 \tag{46}$$

$$\theta_f^*(0,\eta_t,\tau)=-F(\eta_t;0,\tau),\qquad 0<\eta_t<1,\quad \tau>0 \tag{47}$$

$$\left.\frac{\partial\theta_f^*}{\partial\eta_t}\right|_{\eta_t=0}=\frac{3\delta_t(\chi)}{KR}\theta_f^*(\chi,0,\tau),\quad \text{and}\quad \theta_f^*(\chi,1,\tau)=0,\qquad 0<\chi<1,\quad \tau>0 \tag{48}$$

The wall energy equation and the respective conditions are:

$$\begin{aligned}\frac{\partial\theta_{av}(\chi,\tau)}{\partial\tau}=&\frac{R}{Pe_s}\frac{\partial^2\theta_{av}(\chi,\tau)}{\partial\chi^2}+\frac{3}{Pe_sR}[\theta_f^*(\chi,0,\tau)-\theta_{av}(\chi,\tau)]\\ &+\frac{3}{Pe_sR}F(0;\chi,\tau),\qquad 0<\chi<1,\quad \tau>0\end{aligned} \tag{49}$$

$$\theta_{av}(\chi,0)=0,\quad 0<\chi<1 \tag{50}$$

$$\left.\frac{\partial\theta_{av}}{\partial\chi}\right|_{\chi=0}=\left.\frac{\partial\theta_{av}}{\partial\chi}\right|_{\chi=1}=0,\quad \tau>0 \tag{51}$$

Proceeding with application of the GITT [1–5], the proposed auxiliary eigenvalue problem is written as:

$$\begin{aligned}&\frac{d^2\psi(\eta_t)}{d\eta_t^2}+\mu^2\psi(\eta_t)=0,\quad 0<\eta_t<1\\ &\left.\frac{d\psi}{d\eta_t}\right|_{\eta_t=0}=0\ \psi(1)=0\end{aligned} \tag{52}$$

which is readily solved to yield eigenfunctions, eigenvalues and norms, respectively, as:

$$\psi_i(\eta_t)=\cos[\eta_t\mu_i],\qquad 0<\eta_t<1,\quad i=1,2,\ldots \tag{53}$$

$$\mu_i=\frac{(2i-1)\pi}{2},\quad i=1,2,\ldots,$$

$$N_i=\int_0^1\psi_i(\eta_t)\psi_i(\eta_t)\,d\eta_t=1/2 \tag{54}$$

The normalized eigenfunction is given by:

$$\tilde\psi_i(\eta_t)=\frac{\psi_i(\eta_t)}{N_i^{1/2}}=\sqrt{2}\cos[\eta_t\mu_i],\qquad 0<\eta_t<1,\quad i=1,2,\ldots \tag{55}$$

The eigenvalue problem (52) allows definition of the following transform-inverse pair:

$$\bar\theta_{f,j}^*(\chi,\tau)=\int_0^1\tilde\psi_j(\eta_t)\theta_f^*(\chi,\eta_t,\tau)\,d\eta_t\quad\rightarrow\quad \text{Transform} \tag{56}$$

$$\theta_f^*(\chi,\eta_t,\tau)=\sum_{j=1}^{\infty}\tilde\psi_j(\eta_t)\bar\theta_{f,j}^*(\chi,\tau)\quad\rightarrow\quad \text{Inverse} \tag{57}$$

Applying the operator $\int_0^1\tilde\psi_i(\eta_t)\_\_\_\_d\eta_t$ over Eqs. (44), (46) and (47), followed by the inverse formula, then results:

$$\begin{aligned}&\delta_t^2(\chi)\frac{\partial\bar\theta_{f,i}^*(\chi,\tau)}{\partial\tau}+\sum_{j=1}^{\infty}\left[a_{ij}(\chi)\frac{\partial\bar\theta_{f,j}^*(\chi,\tau)}{\partial\chi}+b_{ij}(\chi)\bar\theta_{f,j}^*(\chi,\tau)\right]\\ &\quad=\bar g_i(\chi,\tau),\qquad 0<\chi<1,\quad \tau>0,\quad i=1,2,\ldots\end{aligned} \tag{58}$$

with

$$\begin{aligned}&\bar\theta_{f,i}^*(\chi,0)=-\int_0^1\tilde\psi_i(\eta_t)F(\eta_t;\chi,0)\,d\eta_t\quad\text{and}\\ &\bar\theta_{f,i}^*(0,\tau)=-\int_0^1\tilde\psi_i(\eta_t)F(\eta_t;0,\tau)\,d\eta_t\end{aligned} \tag{59}$$

$$\begin{aligned}a_{ij}(\chi)&=\int_0^1U^*(\chi,\eta_t)\tilde\psi_i(\eta_t)\tilde\psi_j(\eta_t)\,d\eta_t\\ &=\delta_t^2(\chi)\int_0^1U(\eta_t)\tilde\psi_i(\eta_t)\tilde\psi_j(\eta_t)\,d\eta_t\end{aligned} \tag{60}$$

and

$$\begin{aligned}b_{ij}(\chi)=&\frac{6\delta_t(\chi)}{RK}+\frac{1}{Pe_f}\mu_j^2\delta_{ij}+\int_0^1V^*(\chi,\eta_t)\tilde\psi_i(\eta_t)\frac{d\tilde\psi_j(\eta_t)}{d\eta_t}\,d\eta_t\\ \bar g_i(\chi,\tau)=&-\int_0^1\tilde\psi_i(\eta_t)\delta_t^2(\chi)\frac{\partial F(\eta_t;\chi,\tau)}{\partial\tau}\,d\eta_t\\ &-\int_0^1\tilde\psi_i(\eta_t)U^*\frac{\partial F(\eta_t;\chi,\tau)}{\partial\chi}\,d\eta_t\\ &-\int_0^1\tilde\psi_i(\eta_t)V^*\frac{\partial F(\eta_t;\chi,\tau)}{\partial\eta_t}\,d\eta_t\\ &+\int_0^1\tilde\psi_i(\eta_t)\frac{1}{Pe_f}\frac{\partial^2F(\eta_t;\chi,\tau)}{\partial\eta_t^2}\,d\eta_t\end{aligned} \tag{61}$$

The wall heat transfer problem can then be described by a partial differential equation coupled to the transformed fluid temperature fields:

$$\frac{\partial\theta_{av}(\chi,\tau)}{\partial\tau}=\frac{R}{Pe_s}\frac{\partial^2\theta_{av}(\chi,\tau)}{\partial\chi^2}+\frac{3}{Pe_sR}\left[\sum_{j=1}^{\infty}\left[\tilde{\psi}_j(0)\bar{\theta}^*_{f,j}(\chi,\tau)\right]-\theta_{av}(\chi,\tau)\right]+\frac{3}{Pe_sR}F(0;\chi,\tau),\qquad 0<\chi<1,\quad \tau>0 \tag{62}$$

$$\theta_{av}(\chi,0)=0,\quad 0<\chi<1 \tag{63}$$

$$\left.\frac{\partial\theta_{av}}{\partial\chi}\right|_{\chi=0}=\left.\frac{\partial\theta_{av}}{\partial\chi}\right|_{\chi=1}=0,\quad \tau>0 \tag{64}$$

Eqs. (58)–(64) form an infinite coupled system of one-dimensional partial differential equations for the fluid transformed potentials and the average wall temperature. For computational purposes this system is truncated to a sufficiently large finite order, N, for the required convergence control. Once the transformed potentials are numerically computed, the inversion formula, Eq. (57), is employed to reconstruct the filtered potentials, $\theta^*_f(\chi,\eta_t,\tau)$, in explicit form in the transversal coordinate, and after adding the filtering solution, $F(\eta_t;\chi,\tau)$, the dimensionless temperature distribution, $\theta_f(\chi,\eta_t,\tau)$, is recovered everywhere within the boundary layer and along the transient process. Eqs. (58)–(64) in truncated form are then numerically handled by routine *NDSolve* of the *Mathematica* v.5.2 system [33].

The interface condition after the filtering process, Eq. (48), results in a third type boundary condition with variable coefficient. Its incorporation in the adopted eigenvalue problem would produce χ-dependent eigenvalues, eigenfunctions and associated quantities, considerably increasing the analysis effort and computational cost at this phase. For this reason it was preferred to consider a simpler auxiliary problem, similar to the one employed for the case without wall conjugation [8], which avoids the longitudinal coordinate dependence and exactly recovers the second type boundary condition of an imposed wall heat flux.

Due to this choice of a simpler expansion basis, with less information of the original problem, a slower convergence rate of the eigenfunction expansion in the vicinity of the boundary might result. A convergence acceleration technique which is quite adequate to such situations is the so-called Integral Balance approach [1,2], which essentially provides an *a posteriori* convergence enhancement by finding a new inversion formula from the integration of the original partial differential formulation, and substituting the available boundary conditions and the originally proposed inversion formula itself. This technique is based on the concept that the integrals of eigenfunction expansions provide a more favorable convergence behavior than that of the potential expansion itself. Basically, this procedure explicitly incorporates the contribution of the equation and boundary source terms into the improved inversion formula.

The integral balance approach is thus applied by integrating Eq. (44) with $\int_0^1 \_\_\_\,d\eta_t$, which yields:

$$\int_0^1\left[\delta_t^2(\chi)\frac{\partial\theta^*_f(\chi,\eta_t,\tau)}{\partial\tau}+U^*\frac{\partial\theta^*_f(\chi,\eta_t,\tau)}{\partial\chi}+V^*\frac{\partial\theta^*_f(\chi,\eta_t,\tau)}{\partial\eta_t}\right]d\eta_t=\int_0^1\left[\frac{1}{Pe_f}\frac{\partial^2\theta^*_f(\chi,\eta_t,\tau)}{\partial\eta_t^2}+G(\chi,\eta_t,\tau)\right]d\eta_t,\qquad 0<\eta_t<1,\quad 0<\chi<1,\quad \tau>0 \tag{65}$$

Making use of the boundary condition at the edge of the boundary layer, $\left.\frac{\partial\theta^*_f}{\partial\eta_t}\right|_{\eta_{t=1}}=0$, the right-hand side (RHS) of the above expression is given by:

$$\mathrm{RHS}=\int_0^1 G(\chi,\eta_t,\tau)\,d\eta_t-\frac{1}{Pe_f}\left.\frac{\partial\theta_f}{\partial\eta_t}\right|_{\eta_t=0} \tag{66}$$

Applying the original inversion formula given by Eq. (57), to the left-hand side (LRS) of Eq. (65), we find:

$$\mathrm{LHS}=\int_0^1\left[\delta_t^2\frac{\partial}{\partial\tau}\left[\sum_{j=1}^{\infty}\tilde{\psi}_j\bar{\theta}^*_{f,j}\right]+U^*\frac{\partial}{\partial\chi}\left[\sum_{j=1}^{\infty}\tilde{\psi}_j\bar{\theta}^*_{f,j}\right]+V^*\frac{\partial}{\partial\eta_t}\left[\sum_{j=1}^{\infty}\tilde{\psi}_j\bar{\theta}^*_{f,j}\right]\right]d\eta_t$$

Or

$$\mathrm{LHS}=\sum_{j=1}^{\infty}\left[\delta_t^2\left(\int_0^1\tilde{\psi}_j\,d\eta_t\right)\frac{\partial\bar{\theta}^*_{f,j}}{\partial\tau}+\left(\int_0^1U^*\tilde{\psi}_j\,d\eta_t\right)\frac{\partial\bar{\theta}^*_{f,j}}{\partial\chi}+\left(\int_0^1V^*\frac{\partial\tilde{\psi}_j}{\partial\eta_t}\,d\eta_t\right)\bar{\theta}^*_{f,j}\right] \tag{67}$$

Making RHS = LHS, a new expression for the fluid temperature derivative at the interface $\eta_t = 0$ is achieved as:

$$\begin{aligned}\left.\frac{\partial\theta^*_f}{\partial\eta_t}\right|_{\eta_t=0}=&\,Pe_f\int_0^1G(\chi,\eta_t,\tau)\,d\eta_t-Pe_f\\&\times\sum_{j=1}^{\infty}\delta_t^2(\chi)\left(\int_0^1\tilde{\psi}_j(\eta_t)\,d\eta_t\right)\frac{\partial\bar{\theta}^*_{f,j}}{\partial\tau}-Pe_f\\&\times\sum_{j=1}^{\infty}\left(\int_0^1U^*(\chi,\eta_t)\tilde{\psi}_j(\eta_t)\,d\eta_t\right)\frac{\partial\bar{\theta}^*_{f,j}}{\partial\chi}-Pe_f\\&\times\sum_{j=1}^{\infty}\left(\int_0^1V^*(\chi,\eta_t)\frac{\partial\tilde{\psi}_j}{\partial\eta_t}\,d\eta_t\right)\bar{\theta}^*_{f,j}(\chi,\tau)\end{aligned} \tag{68}$$

On the other hand, the solid–fluid interface temperature is also re-evaluated, making use of the above expression and of the interface condition of Eq. (48), to yield the alternative inversion formula below:

$$\begin{aligned}\theta^*_f(\chi,0,\tau)=&\,\frac{KR}{3\delta_t(\chi)}Pe_f\int_0^1G(\chi,\eta_t,\tau)\,d\eta_t\\&-\frac{KR}{3\delta_t(\chi)}Pe_f\sum_{j=1}^{\infty}\delta_t^2(\chi)\left(\int_0^1\tilde{\psi}_j(\eta_t)\,d\eta_t\right)\frac{\partial\bar{\theta}^*_{f,j}}{\partial\tau}\\&-\frac{KR}{3\delta_t(\chi)}Pe_f\sum_{j=1}^{\infty}\left(\int_0^1U^*(\chi,\eta_t)\tilde{\psi}_j(\eta_t)\,d\eta_t\right)\frac{\partial\bar{\theta}^*_{f,j}}{\partial\chi}\\&-\frac{KR}{3\delta_t(\chi)}Pe_f\sum_{j=1}^{\infty}\left(\int_0^1V^*(\chi,\eta_t)\frac{\partial\tilde{\psi}_j}{\partial\eta_t}\,d\eta_t\right)\bar{\theta}^*_{f,j}(\chi,\tau)\end{aligned} \tag{69}$$

The above expressions are expected to provide a sensible improvement on convergence rates with respect to the formal inversion formula previously presented.

4. Results and discussion

The developed *Mathematica* code [33] incorporates all the symbolic and numerical computational steps in the solution procedure. This notebook was validated in several ways, including comparisons with the Blasius solution for the thermal boundary layer for steady state and without wall conjugation [34], and against the transient solution with the Karman–Pohlhausen integral method approximation [26]. The improved lumped formulation was also validated and inspected by solving the two-dimensional heat conduction equation at the wall, employing the here obtained interface temperature as a boundary condition. More details on this validation effort can be found in Ref. [27]. Here, we first report part of the numerical analysis performed to inspect the local error

control of the NDSolve routine [33] in the numerical solution of the coupled partial differential system, and the global error control through the convergence of the eigenfunction expansions, as recommended in the proposed hybrid numerical–analytical solution. Then, we proceed towards the physical interpretation of the conjugation effect along the transient behavior. On the basis of the flash experiment motivation [25,26], five test cases with wall conjugation were considered, for three different materials (Norcoat, PVC and aluminum) and respective plate thicknesses, as detailed in Table 1. The base case (case 0) is related to the situation without wall conjugation, already treated in Ref. [8] by the same hybrid approach.

Air was always the cooling fluid and the adopted numerical values in the simulations for the related governing parameters were:

$$L = 0.1\ \text{m}, \quad u_\infty = 1\ \text{m/s}, \quad T_\infty = 20\ ^\circ\text{C},$$
$$\alpha_f = 2.22 \times 10^{-5}\ \text{m}^2/\text{s}, \quad k_f = 0.0262\ \text{W}/(\text{m}\,^\circ\text{C}),$$
$$\nu = 1.57 \times 10^{-5}\ \text{m}^2/\text{s}, \quad \phi_{ref} = 100\ \text{W/m}^2$$

In the numerical analysis of the code we have mostly employed case no. 2, for a Norcoat wall of 7 mm thickness, and for a time step with a uniform heat flux incidence at the fluid–solid interface, $\phi(t) = \phi_{ref}$, $Q_w(t) = 1$. Table 2 illustrates the numerical behavior of the interface temperature for case 2, at different time values and for the longitudinal positions $x^* = 0.01$ and 0.1 m, by varying the parameter MaxStepSize of routine NDSolve [33], which controls the maximum allowable step size in the discretization procedure of the Method of Lines. Clearly, the default operation mode in this built in routine cannot provide an uniform error control over the whole solution domain. However, the user might directly control the computations by varying this parameter and inspecting the relative errors achieved. For instance, at least four digits precision is reached within the range of MaxStepSize here investigated for both the spatial and time variables ($\Delta x = 0.002$ and $\Delta t = 0.025$).

Next, we demonstrate the convergence rates achievable by the chosen eigenfunction expansion in combination with the proposed integral balance approach. A brief convergence analysis for case 2 is illustrated in Table 3, by varying the truncation order in the series representation for the temperature field at the interface. Table 3 illustrates, for two values of the time variable, $t = 0.2$ s and $t = 2$ s, the interface temperature convergence, according to Eq. (69), for three different positions along the plate.

Clearly, full convergence to six significant digits is achieved in all cases, with truncation orders less than $N = 20$. Also, with much lower truncation orders, $N < 10$, an impressive convergence to ±1 in the fourth significant digit is obtainable throughout the considered range of the independent variables.

The physical conjugated problem is now analyzed by considering all six cases described in Table 1, including the situation without wall conjugation (case 0) as a reference state. Fig. 2a–f thus presents the time evolution of the fluid–solid interface temperatures at different longitudinal positions, $x = 0.01$, 0.025, 0.05, 0.075, and 0.1 m, within appropriate ranges for the time variable for each case. The arrows indicate the sense of increasing longitudinal positions for the various curves shown. In fact, the first observation comes from the dramatically different time ranges achieved in each of the cases analyzed. The transient convection problem without wall conjugation already reaches steady state for all of the plate length within a fraction of a second, while the two last cases (Fig. 2e and f) of materials with large thermal capacities, and larger thicknesses, require a few hours for reaching a steady situation. For the same material (Norcoat) and increasing wall thicknesses (Fig. 2b–d), the longer transient is also observable, though still within the range of a few seconds, due to low thermal

Table 1
Test cases and governing parameters

Case	Material	e (m)	k_s (W/m °C)	$(\rho c_p)_s$ (J/m^3 °C)	α_s (m^2/s)
0	No conjugation	–	–		–
1	Norcoat	0.002	0.12	718.6	1.67×10^{-4}
2	Norcoat	0.007	0.12	718.6	1.67×10^{-4}
3	Norcoat	0.012	0.12	718.6	1.67×10^{-4}
4	PVC	0.012	0.15	$1.36 \times 10^{+6}$	0.11×10^{-6}
5	Aluminum	0.012	238	$2.55 \times 10^{+6}$	9.33×10^{-5}

Table 3
Convergence behavior of the interface temperature expansion for different truncation orders, according to the integral balance expression, Eq. (69), at $t = 0.2$ and 2.0 s

GITT + integral balance							
$t = 0.2$ s				$t = 2.0$ s			
Number of terms	Interface temperature (°C)			Number of terms	Interface temperature (°C)		
	$x = L/10$	$x = L/2$	$x = L$		$x = L/10$	$x = L/2$	$x = L$
1	22.5450	23.7543	24.0676	1	23.8715	28.6060	31.5838
2	22.6227	23.7818	24.0905	2	24.0351	28.7891	31.7553
3	22.6016	23.7642	24.0696	3	23.9839	28.7394	31.7803
4	22.6028	23.7704	24.0794	4	23.9931	28.7450	31.7329
5	22.6008	23.7668	24.0753	5	23.9875	28.7404	31.7508
6	22.6012	23.7687	24.0777	6	23.9894	28.7416	31.7374
7	22.6006	23.7675	24.0764	7	23.9878	28.7403	31.7436
8	22.6008	23.7683	24.0773	8	23.9885	28.7408	31.7388
9	22.6006	23.7677	24.0767	9	23.9879	28.7403	31.7415
10	22.6006	23.7681	24.0771	10	23.9882	28.7405	31.7393
11	22.6005	23.7678	24.0768	11	23.9879	28.7403	31.7406
12	22.6006	23.7681	24.0771	12	23.9881	28.7404	31.7395
13	22.6005	23.7679	24.0769	13	23.9879	28.7403	31.7402
14	22.6006	23.7680	24.0770	14	23.9880	28.7403	31.7395
15	22.6005	23.7679	24.0769	15	23.9879	28.7403	31.7400
16	22.6005	23.7680	24.0770	16	23.9880	28.7403	31.7396
17	22.6005	23.7679	24.0769	17	23.9879	28.7402	31.7399
18	22.6005	23.7680	24.0770	18	23.9880	28.7403	31.7396
19	22.6005	23.7679	24.0770	19	23.9879	28.7402	31.7399
20	22.6005	23.7680	24.0770	20	23.9879	28.7403	31.7396

Table 2
Numerical behavior of the interface temperature for different values of the error control parameter (MaxStepSize) in the routine NDSolve [33]

Interface temperature (°C): $x = 0.01$ m					Interface temperature (°C): $x = 0.1$ m				
t (s)	MaxStepSize				t (s)	MaxStepSize			
	Default	x: 0.002 t: 0.1	x: 0.002 t: 0.05	x: 0.002 t: 0.025		Default	x: 0.002 t: 0.1	x: 0.002 t: 0.05	x: 0.002 t: 0.025
0.02	21.4953	21.4956	21.4956	21.4958	0.02	21.9869	21.9872	21.9872	21.9873
0.04	21.6597	21.6571	21.6581	21.6591	0.04	22.2751	22.2740	22.2747	22.2753
0.06	21.8133	21.8065	21.8087	21.8103	0.06	22.5556	22.5529	22.5545	22.5555
0.08	21.9569	21.9452	21.9485	21.9505	0.08	22.8284	22.8242	22.8267	22.8282
0.1	22.0911	22.0742	22.0783	22.0807	0.1	23.0939	23.0882	23.0915	23.0934
0.2	22.6437	22.6018	22.6068	22.6097	0.2	24.3173	24.3074	24.3128	24.3159
0.3	23.0432	22.9822	22.9856	22.9876	0.3	25.3834	25.3747	25.3793	25.3820

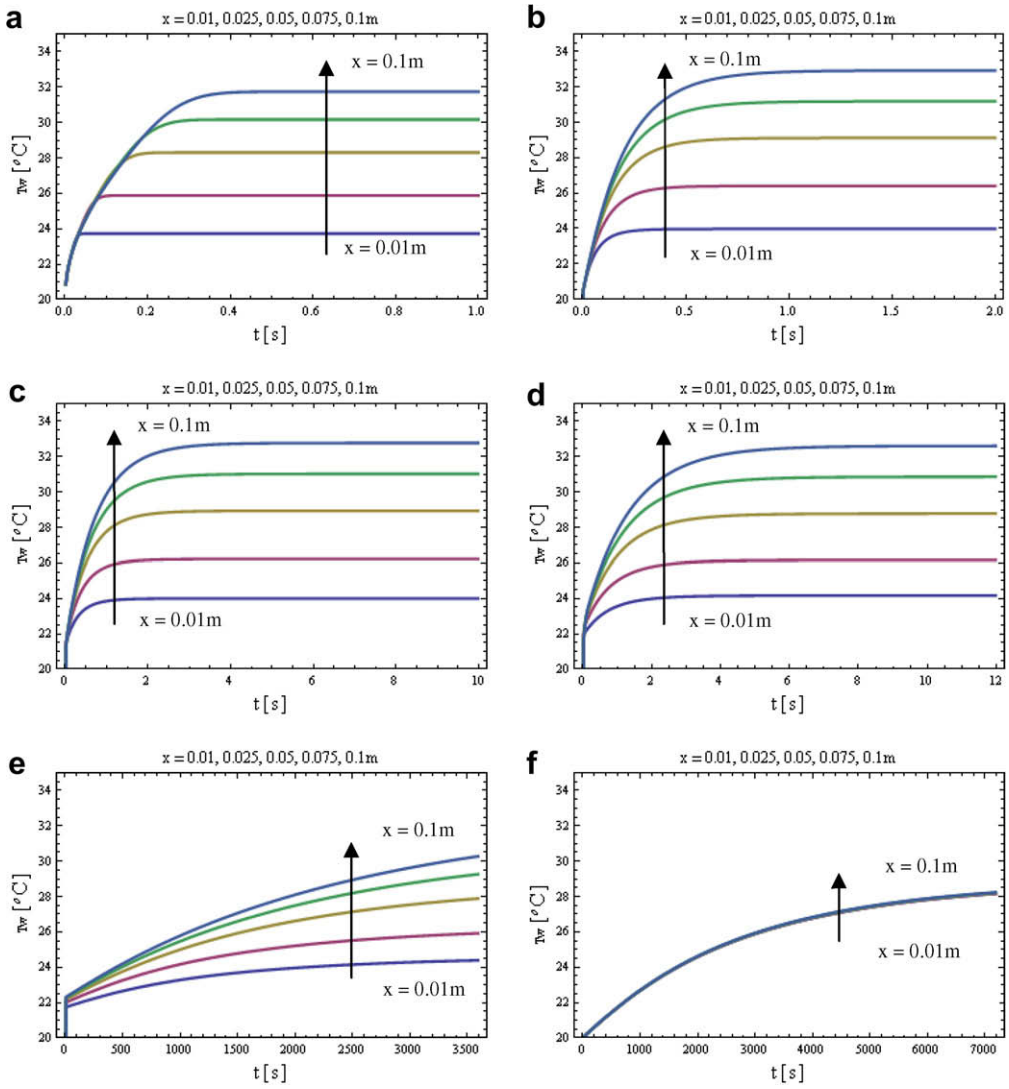

Fig. 2. Transient behavior of interface temperatures at selected longitudinal positions and for different wall materials and thicknesses. (a) Case 0: without conjugation; (b) case 1: Norcoat 2 mm; (c) case 2: Norcoat 7 mm; (d) case 3: Norcoat 12 mm; (e) case 4: PVC 12 mm; and (f) case 5: aluminum 12 mm.

capacitance of this material. In addition, it is clear that the steady state is achieved earlier for those positions closer to the leading edge of the plate in all cases, though this is not so evident in the aluminum case (Fig. 2f) when the interface temperature distribution is practically spatially uniform, in light of the high thermal conductivity and effective heat diffusion along the plate length. Superposition of any of the cases with wall conjugation over the base case of no wall participation, clearly confirm the non-negligible effect in the transient and spatial behavior of the interface temperatures.

One important aspect in this situation of an applied known heat flux at the solid–fluid interface, is to quantify the heat flux partition between the solid and the fluid along the plate length and with time, which is indeed quite different from the behavior in the more usual situation of an imposed heat flux at the wall face not in contact with the exchanging fluid. Fig. 3a–f thus presents the heat fluxes to the solid (solid lines, lower curves in each graph) and to the fluid (dashed lines, upper curves) in each case, plotted against the longitudinal coordinate and for different values of the time variable as pointed out above the graph, starting from the base case when all the imposed heat is directly delivered to the fluid at each position ($\phi = 100\ \mathrm{W/m^2}$). The arrows indicate the sense of increasing time variable value for the various curves shown. It is first evident from all of the graphs presented, that the employed boundary layer formulation leads to the expected singularity at the leading edge, where the heat transfer coefficient becomes infinite. One may see that along the time variable the heat flux to the fluid is increasing, while to the solid it should be decreasing, in light of the smoother temperature gradients across the wall. Along the plate length, the heat flux to the fluid decreases, following the heat transfer coefficient behavior, which is very high close to the plate edge singularity. One may also observe, more clearly from the last two cases, Fig. 3e and f, that it might exist a turning point along the plate length, when the heat flux to the solid switches sense, closer to the plate leading edge and increasing its position along the transient process. Thus, for positions further away from the leading edge, the imposed heat flux is partitioned between the fluid and the solid, while for positions closer to the plate leading edge some additional heat from the solid may be removed by the fluid, as illustrated in Fig. 4, with the net heat flow along the plate length in the negative x sense. In all cases shown here we have verified that the summation of the two heat fluxes at each position, equals the applied flux at the interface. In the last two cases, Fig. 3e and f, one may observe that the two heat fluxes

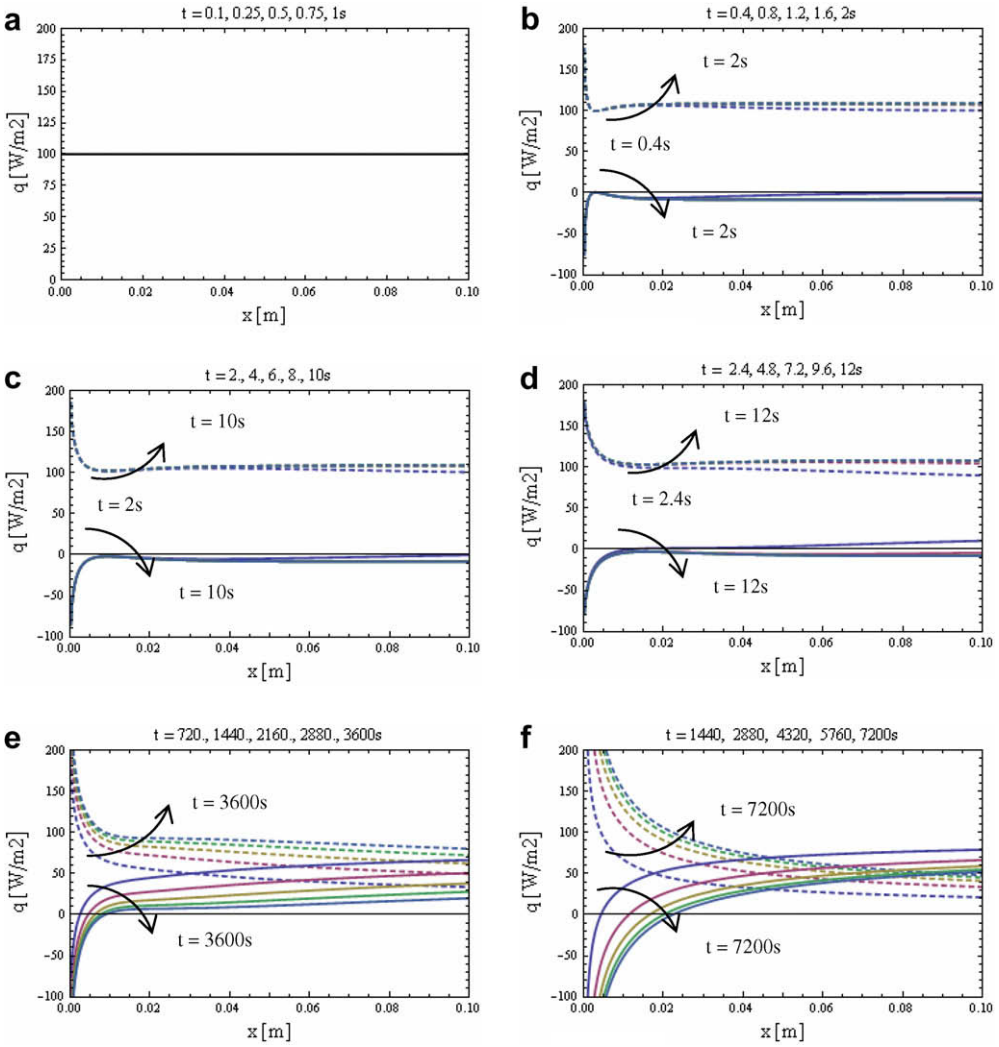

Fig. 3. Longitudinal variation of partitioned heat fluxes to the solid and to the fluid along the interface at selected values of time and for different wall materials and thicknesses (dashed lines, heat flux to the fluid; solid lines, heat flux to the solid). (a) Case 0: without conjugation; (b) case 1: Norcoat 2 mm; (c) case 2: Norcoat 7 mm; (d) case 3: Norcoat 12 mm; (e) case 4: PVC 12 mm; and (f) case 5: aluminum 12 mm.

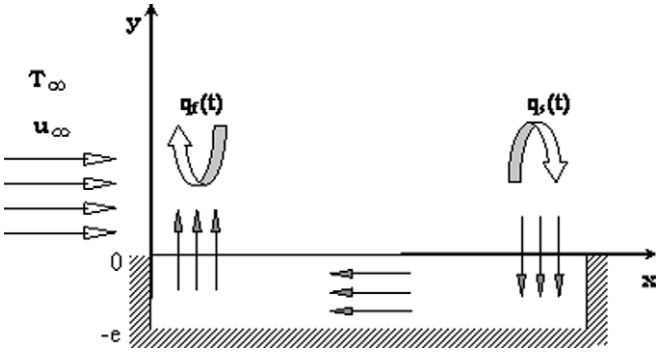

Fig. 4. Illustration of the heat flux partition and the wall conjugation effect.

cross at a certain longitudinal position, after which the wall starts retrieving more energy than the fluid from the incident heat flux at that particular position. As the steady state is approached the integral of the wall heat flux along the longitudinal coordinate tends to zero, since all the other boundaries are insulated and the internal energy within the solid ceases changing with time, while the integral of the fluid heat flux over the plate surface recovers, in full, the total delivered heat transfer rate. We may again observe the typically slower transients, from these two situations, cases 4 and 5, due to the much higher thermal capacitance in comparison to the Norcoat wall, cases 1–3, as demonstrated by the heat flux partition evolutions presented in Fig. 3.

Fig. 5a–f illustrates the transient behavior of the local heat transfer coefficients for each of the six cases, for the same selected longitudinal positions as in Fig. 2. The arrows indicate the sense of increasing longitudinal positions for the various curves shown. It is clear, in all cases, that steady-state values for the heat transfer coefficients are reached much before than for either the interface temperatures or heat fluxes. Such behavior permits the construction of approximate transient solutions based on constant heat transfer coefficient values along the transients, but one should be careful in adopting the appropriate correlations for the Nusselt number, since wall conjugation markedly affects the spatial variation of the heat transfer coefficients, as observable from Fig. 5. For instance, the heat transfer coefficient for case 5, the aluminum wall, is more closely approximated by the situation of a prescribed uniform wall temperature, while case 2 for the thinner Norcoat wall is more appropriately approximated by an imposed uniform wall heat flux. This aspect is more clearly illustrated in Fig. 6, which presents the steady-state longitudinal distribution of the

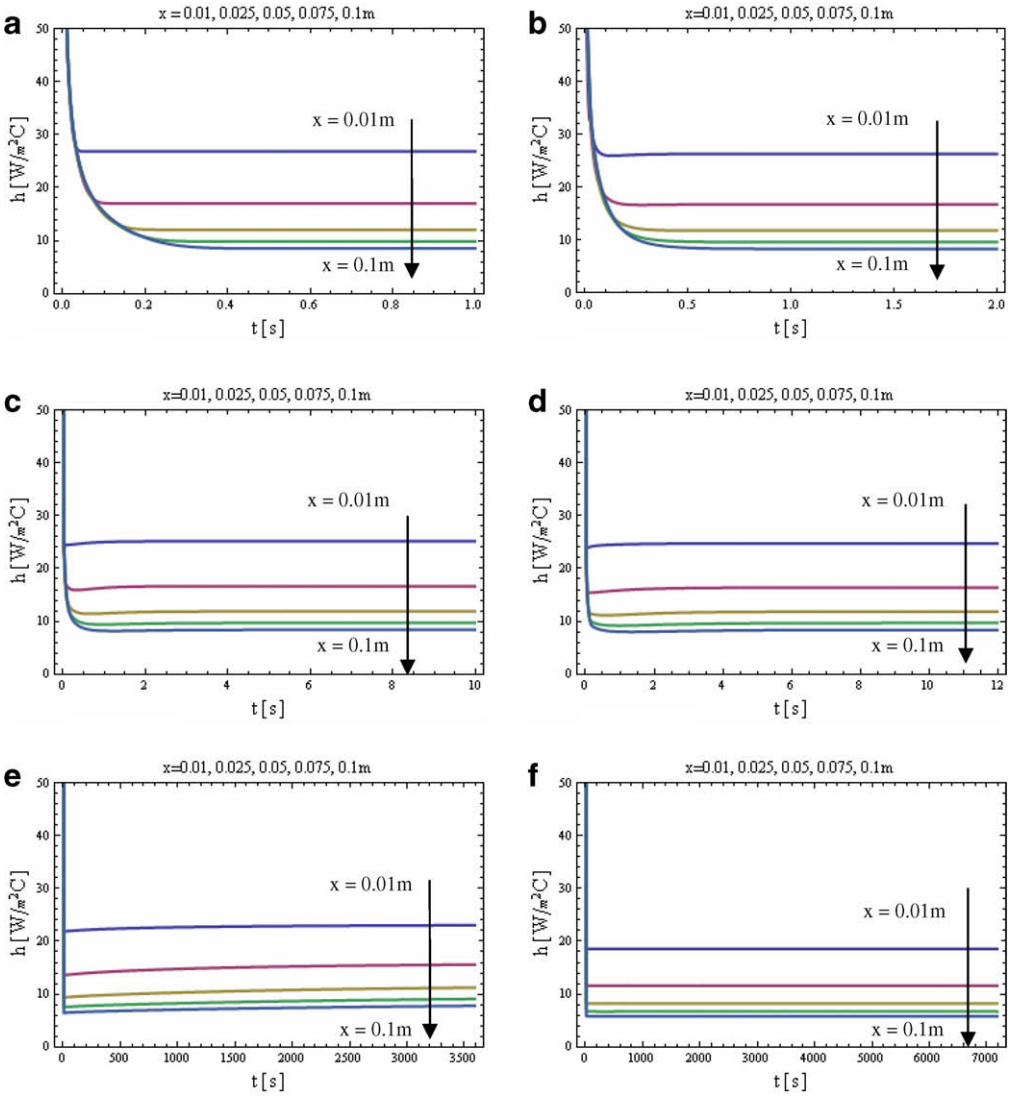

Fig. 5. Transient behavior of local heat transfer coefficients at selected longitudinal positions and for different wall materials and thicknesses. (a) Case 0: without conjugation; (b) case 1: Norcoat 2 mm; (c) case 2: Norcoat 7 mm; (d) case 3: Norcoat 12 mm; (e) case 4: PVC 12 mm; and (f) case 5: aluminum 12 mm.

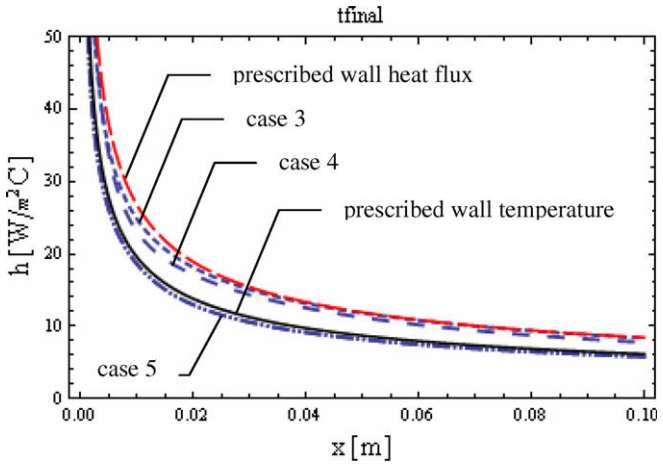

Fig. 6. Steady-state behavior of local heat transfer coefficients along the longitudinal coordinate for different wall materials and same thickness (12 mm), cases 3–5, as compared to theoretical correlations without conjugation for prescribed wall temperature (lower solid line) and prescribed wall heat flux (upper line).

local heat transfer coefficient, as obtained for the three materials here considered, Norcoat, PVC and aluminum, for the same wall thickness of 12 mm (cases 3, 4 and 5). Case 3 is shown in short dashed line, case 4 in long dashed line, while case 5 is in dot-dashed line. In addition, the results from the classical theoretical correlations for both the prescribed temperature and prescribed heat flux boundary conditions, without wall conjugation, are presented in solid lines (lower curve is for the first kind condition). As we can see, the Norcoat results (case 3) are the ones closer to the prescribed heat flux behavior, followed by the PVC wall (case 4), while the aluminum case (case 5) is indeed much closer to a prescribed wall temperature physical problem.

Fig. 7 illustrates the transient behavior of both the wall temperature (Fig. 7a) and the local heat transfer coefficient (Fig. 7b), for the three different thicknesses of Norcoat (cases 1–3), at the position $x = 0.1$ (end of the plate). Clearly, the wall temperatures experience a much longer transient behavior, as observed above, changing along approximately 6 s, while the heat transfer coefficient ceases to change at less than 0.5 s. It should be noted that the time scales of the two graphs are actually different for clarity in Fig. 7a and b. Also, significant differences in the wall tempera-

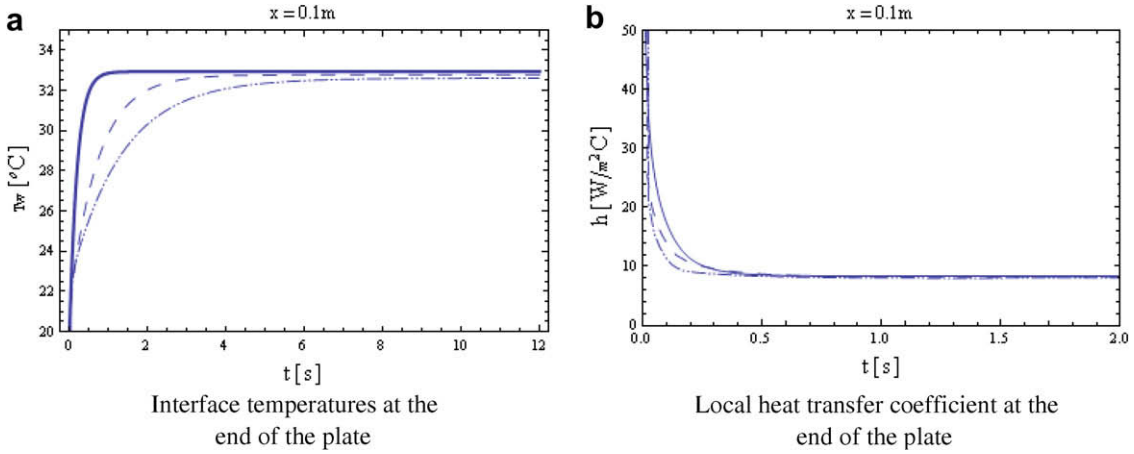

Fig. 7. Comparison of the transient behavior of the interface temperature and local heat transfer coefficients for different wall thicknesses of Norcoat, case 1 (2 mm): solid lines; case 2 (7 mm): dashed lines; case 3 (12 mm): dot-dashed lines. (a) Interface temperatures at the end of the plate. (b) Local heat transfer coefficient at the end of the plate.

ture behavior due to the varying thickness are observable essentially along the transient period, in light of the relevant thermal capacitance difference, while the steady values for both the wall temperature and heat transfer coefficients are not markedly apart for the three wall thicknesses.

5. Conclusions

The present work was concerned with the solution and physical interpretation of a transient conjugated conduction–external convection problem, for laminar flow over a flat plate of non-negligible thickness, with heat flux being delivered at the fluid–wall interface. The wall heat conduction problem was first simplified, by making use of the coupled integral equations approach to find an improved lumped-differential formulation for the transversally averaged wall temperature, as a function of the time variable and of the longitudinal coordinate. Then, the GITT was applied to the resulting formulation in its partial transformation mode, i.e., by removing only the transversal coordinate through the integral transformation of the fluid energy equation. A system of partial differential equations is thus obtained, coupling the transformed fluid temperatures and average wall temperature, which is then numerically solved by the Method of Lines implemented in the *Mathematica* package. All of the analytical steps in the methodology derivation were also incorporated into the developed mixed symbolic–numerical computer code.

The proposed combination of problem reformulation and hybrid solution methodology were demonstrated to be accurate and robust from the numerical point of view. It was also pointed out that care must be exercised when employing the Method of Lines routine in its automatic error control mode, since numerical loss of accuracy and oscillations were observed for short times and longitudinal positions very close to the plate edge singularity. Numerical results for interface temperature, heat transfer coefficient and heat flux partition are reported for six different physical situations of wall participation, illustrating the importance of considering this phenomena in most cases. The developed approach is also fairly flexible so as to accommodate any form of the imposed interface heat flux variation in both position and time, and should be extendable to various other physical situations, as motivated by future applications.

Acknowledgements

The authors (R.M.C. and C.P.N.) acknowledge the kind hospitality of the Laboratoire de Thermomécanique, LTM, Université de Reims, France, during their stay in January and February, 2008. This work was also partially supported by CNPq/Brasil and CNRS/France.

References

[1] R.M. Cotta, Integral Transforms in Computational Heat and Fluid Flow, CRC Press, Boca Raton, FL, 1993.
[2] R.M. Cotta, M.D. Mikhailov, Heat Conduction: Lumped Analysis, Integral Transforms, Symbolic Computation, Wiley–Interscience, New York, 1997.
[3] R.M. Cotta, The Integral Transform Method in Thermal and Fluids Sciences and Engineering, Begell House, New York, 1998.
[4] C.A.C. Santos, J.N.N. Quaresma, J.A. Lima, Benchmark Results for Convective Heat Transfer in Ducts: The Integral Transform Approach, ABCM Mechanical Sciences Series, Editora E-Papers, Rio de Janeiro, 2001.
[5] R.M. Cotta, M.D. Mikhailov, Hybrid methods and symbolic computations, in: W.J. Minkowycz, E.M. Sparrow, J.Y. Murthy (Eds.), Handbook of Numerical Heat Transfer, second ed., Wiley, New York, 2006, pp. 493–522 (Chapter 16).
[6] M.A.H. Bolivar, P.L.C. Lage, R.M. Cotta, Integral transform solution of the laminar thermal boundary layer problem for flow past two-dimensional and axisymmetric bodies, Numer. Heat Transfer Part A 33 (7) (1998) 779–797.
[7] Jian Su, On the integral transform solution of laminar boundary layers with distributed suction, Hybrid Methods Eng. 1 (2) (1999) 103–118.
[8] C.P. Naveira, M. Lachi, R.M. Cotta, J. Padet, Integral transform solution of transient forced convection in external flow, Int. Commun. Heat Mass Transfer 34 (2007) 703–712.
[9] R.M. Cotta, J.E.V. Gerk, Mixed finite difference/integral transform approach for parabolic–hyperbolic problems in transient forced convection, Numer. Heat Transfer Part B 25 (1994) 433–448.
[10] F.V. Castellões, R.M. Cotta, Analysis of transient and periodic convection in microchannels via integral transforms, Prog. Comput. Fluid Dynamics 6 (6) (2006) 321–326.
[11] M. Lachi, R.M. Cotta, C.P. Naveira, J. Padet, Solution hybride dans l'étude de la convection forcée externe, Proc. of the Congrès Français de Thermique, SFT 2006, Actes T. 1, Ile de Ré, France, May, 2006, pp. 373–378.
[12] Y.L. Perelman, On conjugate problems of heat transfer, Int. J. Heat Mass Transfer 3 (1961) 293–303.
[13] A.V. Luikov, V.A. Aleksashenko, A.A. Aleksashenko, Analytical methods of solution of conjugated problems in convective heat transfer, Int. J. Heat Mass Transfer 14 (1971) 1047–1056.
[14] A.V. Luikov, Conjugate convective heat transfer problems, Int. J. Heat Mass Transfer 17 (2) (1974) 257–265.
[15] A. Pozzi, M. Lupo, The coupling of conduction with forced convection over a flat plate, Int. J. Heat Mass Transfer 32 (1989) 1207–1214.
[16] I. Pop, D.B. Ingham, A note on conjugated forced convection boundary layer flow past a flat plate, Int. J. Heat Mass Transfer 36 (1993) 3873–3876.
[17] M. Vynnycky, S. Kimura, K. Kanev, I. Pop, Forced convection heat transfer from a flat plate: the conjugate problem, Int. J. Heat Mass Transfer 41 (1998) 45–59.
[18] M. Mossad, Laminar forced convection conjugate heat transfer over a flat plate, Heat Mass Transfer 35 (1999) 371–375.
[19] A. Pozzi, R. Tognaccini, Coupling of conduction and convection past an impulsively started semi-infinite flat plate, Int. J. Heat Mass Transfer 43 (2000) 1121–1131.
[20] K. Chida, Surface temperature of a flat plate of finite thickness under conjugate laminar forced convection heat transfer condition, Int. J. Heat Mass Transfer 43 (2000) 639–642.

[21] R.O.C. Guedes, R.M. Cotta, N.C.L. Brum, Heat transfer in laminar tube flow with wall axial conduction effects, J. Thermophys. Heat Transfer 5 (4) (1991) 508–513.
[22] R.O.C. Guedes, R.M. Cotta, Periodic laminar forced convection within ducts including wall heat conduction effects, Int. J. Eng. Sci. 29 (5) (1991) 535–547.
[23] R.O.C. Guedes, R.M. Cotta, M.N. Özisik, Conjugated periodic turbulent forced convection in a parallel plate channel, J. Heat Transfer 116 (1994) 40–46.
[24] M. Lachi, M. Rebay, E. Mladin, J. Padet, Integral approach of the transient coupled heat transfer over a plate exposed to a variation in the input heat flux, in: ICHMT International Symposium Transient Convective Heat and Mass Transfer in Single & Two-Phase Flows, August, Cesme, Turkey, 2003.
[25] M. Lachi, J. Padet, M. Rebay, R.M. Cotta, Numerical solution for transient thermal interaction between a laminar boundary layer flow and a flat plate, in: Proceedings of 10th Brazilian Congress of Thermal Sciences and Engineering, ENCIT 2004, Rio de Janeiro, Brasil, November–December, 2004.
[26] M. Lachi, R.M. Cotta, C.P. Naveira, J. Padet, Improved lumped-differential formulation of transient conjugated conduction–convection in external flow, in: 11th Brazilian Congress of Thermal Sciences and Engineering, ENCIT 2006, Curitiba, Brasil, Paper No. CIT06-0965, December, 2006.
[27] Naveira, C.P., R.M. Cotta, M. Lachi, J. Padet, Transient conjugated conduction–external convection with front face imposed wall heat flux, in: Proceedings of IMECE2007, ASME International Mechanical Engineering Congress & Exposition, Paper No. IMECE2007-41417, Seattle, Washington, USA, November 11–15, 2007.
[28] M. Remy, A. Degiovanni, D. Maillet, Mesure de coefficient d'échange pour des écoulements à faible vitesse, Rev. Gén. Therm. 397 (1995) 28–42.
[29] M. Rebay, M. Lachi, J. Padet, Mesure de coefficients de convection par méthode impulsionnelle – influence de la perturbation de la couche limite, Int. J. Therm. Sci. 41 (2002) 1161–1175.
[30] J.B. Aparecido, R.M. Cotta, Improved one-dimensional fin solutions, Heat Transfer Eng. 11 (1) (1989) 49–59.
[31] R.M. Cotta, M.N. Ozisik, J. Mennig, Coupled integral equation approach for phase-change problem in two-regions finite slab, J. Franklin Inst. 327 (2) (1990) 225–234.
[32] E.J. Correa, R.M. Cotta, Enhanced lumped-differential formulations of diffusion problems, Appl. Math. Model. 22 (1998) 137–152.
[33] S. Wolfram, The Mathematica Book, fourth ed., Wolfram Media, Cambridge, 1999.
[34] F.M. White, Viscous Fluid Flow, McGraw-Hill, New York, 1974.